XIV International Conference on Computational Plasticity. Fundamentals and Applications
COMPLAS XIV
E. Oñate, D.R.J. Owen, D. Peric & M. Chiumenti (Eds)

A THERMODYNAMICALLY CONSISTENT COHESIVE DAMAGE MODEL FOR THE SIMULATION OF MIXED-MODE DELAMINATION

FEDERICA CONFALONIERI* AND UMBERTO PEREGO*

* Department of Civil and Environmental Engineering
Politecnico di Milano
Piazza Leonardo da Vinci, 32, Milano, Italy
e-mail: federica.confalonieri@polimi.it - umberto.perego@polimi.it

Key words: Mixed-mode delamination, cohesive model, isotropic damage

Abstract. This work is devoted to the formulation of a new cohesive model for mixed-mode delamination. The model is based on a thermodynamically consistent isotropic damage formulation, with consideration of an internal friction mechanism that governs the interaction between normal and shear opening modes.

1 INTRODUCTION

Delamination, i.e. the progressive decohesion between two layers, is one of the main causes of failure for laminated composites. Delamination often develops under the presence of concurrent interlaminar tensile and shear stresses, leading to mixed-mode loading conditions with variable mode ratios. Several experimental works [1, 2, 3] have shown that the micro-mechanical mechanisms involved in the delamination phenomenon vary with the mixed-mode ratio, with a transition from pure mode I loading characterized by matrix cleavage and fiber pull-out, to mode II conditions dominated by the formations of cusps and hackles. At the macroscopic scale, this causes the fracture energy to increase in passing from Mode I to Mode II, as confirmed by results of experimental tests performed on many different composite materials (see, for instance, [4, 5]). As an example, Figure 1 shows the values of fracture energy at different mode ratios reported in [6] and deriving from different experiments performed with the Mixed Mode Bending test apparatus [7] on AS4/3501-6 carbon/epoxy composite. Empirical relationships have been proposed in the literature to define a failure locus able to interpolate the toughness variation over the full mixed-mode range. Among them, it is worth mentioning the Power Law [8] and the BK law [4], widely employed as delamination criteria.

Robust numerical simulation tools are mandatory to obtain accurate predictions of the onset and propagation of delamination in real-life problems, characterized by variable loading paths. The finite element simulation of the decohesion between layers is often addressed by means of interface elements, whose constitutive behavior is modeled by a

ISBN:978-84-946909-6-9

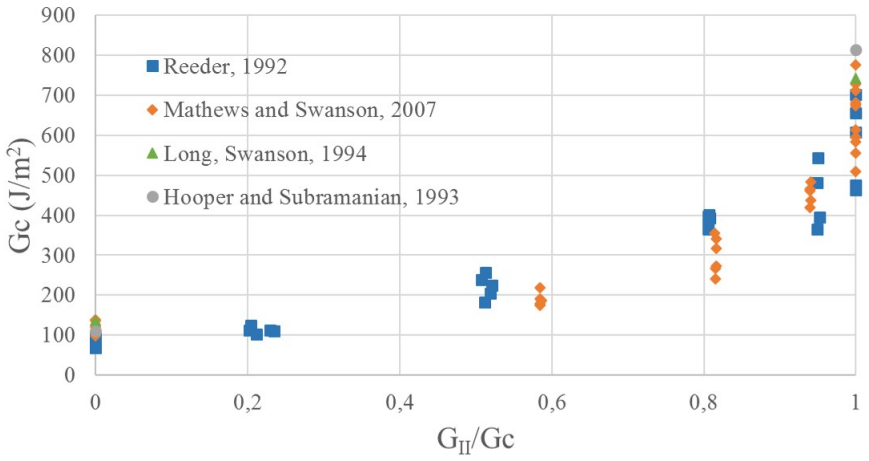

Figure 1: AS4/3501-6: fracture energy vs mode mixity

cohesive law. In the literature, one can find a huge number of works on the cohesive modeling of delamination, (see, for instance, [9, 10, 11]). However, many of them exhibit some limitations, such as the need of assumptions on the loading path, the lack of thermodynamic consistency, or the inability to ensure the correct energy dissipation in case of non-proportional loading paths. These drawbacks may affect the reliability of the numerical results when mixed-mode loading conditions with variable mode mixity ratios and/or non-proportional loading are considered.

This work proposes a new cohesive model, based on a thermodynamically consistent formulation with isotropic damage. An internal friction parameter is introduced to handle the coupling between normal and shear stresses. The overall fracture energy at any mode ratio is an outcome of the model, without the need to introduce any empirical laws to define the fracture energy variation with the mode-mixity ratio.

2 FORMULATION

Let us consider the zero-thickness 2D interface element with four nodes shown in Figure 2. Under the hypothesis of small openings, the relative displacement vector $\boldsymbol{\delta}$ is computed as the difference between the displacements of two corresponding points belonging to the top and bottom edges respectively:

$$\boldsymbol{\delta} = \boldsymbol{\delta}^{+} - \boldsymbol{\delta}^{-} \tag{1}$$

A local reference frame is introduced in order to identify the normal and the tangential directions. Superscripts n and s will denote the normal and the shear components, respectively, of tractions and opening displacements.

The starting point of the formulation is the introduction of the free energy per unit surface Ψ, defined as:

$$\Psi = \frac{1}{2} K \left(\langle \delta^n \rangle_-\right)^2 + \frac{1}{2} \left(1-d\right) K \left(\langle \delta^n \rangle_+\right)^2 + \frac{1}{2} \left(1-d\right) K \left(\delta^s\right)^2 \tag{2}$$

where K is the elastic stiffness of the interface and d the isotropic damage variable.

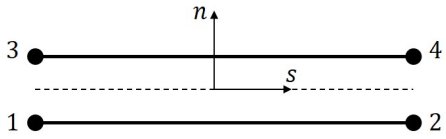

Figure 2: 4-node interface element

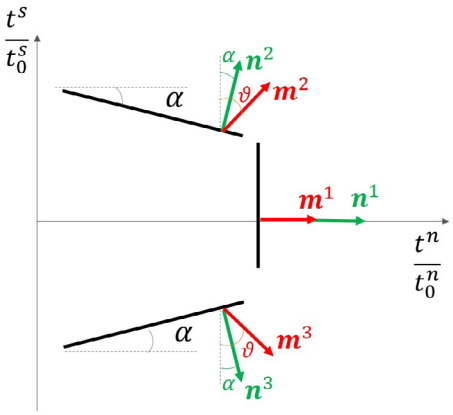

Figure 3: Damage modes

The same elastic stiffness is considered in the normal and in the shear directions. The Macauley brackets $\langle\ \rangle$ are introduced to distinguish between the negative and the positive part of the normal opening displacement, so that the unilateral effect is accounted for. The cohesive tractions t^n and t^s and the strain energy release rate Y per unit damage growth are obtained through the state equations:

$$t^n = \frac{\partial \Psi}{\partial \delta^n} = K\langle\delta^n\rangle_- + (1-d)\,K\langle\delta^n\rangle_+ \qquad t^s = \frac{\partial \Psi}{\partial \delta^s} = (1-d)\,K\delta^s \tag{3}$$

$$Y = -\frac{\partial \Psi}{\partial d} = \tfrac{1}{2}K\left(\langle\delta^n\rangle_+\right)^2 + \tfrac{1}{2}K\left(\delta^s\right)^2 \tag{4}$$

For the sake of simplicity, in the following only the tensile case, i.e. $\delta^n \geq 0$, will be considered.

The model is based on the definition of three different damage modes in the plane of non-dimensional cohesive tractions, identified by the normal unit vectors $\mathbf{n^1}$, $\mathbf{n^2}$ and $\mathbf{n^3}$ (see Figure 3), whose interaction governs the cohesive interface evolution under mixed-mode loading conditions. As can be seen from Figure 3, $\mathbf{n^1}$ defines the opening-dominated mode, while $\mathbf{n^2}$ and $\mathbf{n^3}$ the two shear-dominated modes. The three normals are collected in matrix $\mathbf{N}$:

$$\mathbf{N} = \begin{bmatrix} \mathbf{n^1} \\ \mathbf{n^2} \\ \mathbf{n^3} \end{bmatrix} = \begin{bmatrix} 1 & 0 \\ \sin\alpha & \cos\alpha \\ \sin\alpha & -\cos\alpha \end{bmatrix} \tag{5}$$

where the angle α, playing the role of a parameter of internal friction, defines the inclination of the two shear-dominated damage modes.

A vector of effective cohesive stresses $\mathbf{s} = [s^1\ s^2\ s^3]^T$ is defined by projecting the vector of dimensionless cohesive traction $\overline{\mathbf{t}}$ along the three normals:

$$\mathbf{s} = \mathbf{N}\overline{\mathbf{t}} \tag{6}$$

where:

$$\overline{\mathbf{t}} = \begin{bmatrix} \overline{t}^n \\ \overline{t}^s \end{bmatrix} = \begin{bmatrix} \frac{t^n}{t_0^n} \\ \frac{t^s}{t_0^s} \end{bmatrix} \tag{7}$$

being t_0^n and t_0^s the strengths in pure Modes I and II. Thus, eqn. 6 becomes:

$$\begin{aligned} s^1 &= \overline{\mathbf{t}}^T\mathbf{n^1} = \overline{t}^n \\ s^2 &= \overline{\mathbf{t}}^T\mathbf{n^2} = \overline{t}^n\sin\alpha + \overline{t}^s\cos\alpha \\ s^3 &= \overline{\mathbf{t}}^T\mathbf{n^3} = \overline{t}^n\sin\alpha - \overline{t}^s\cos\alpha \end{aligned} \tag{8}$$

Let us now introduce the effective opening displacements $\mathbf{w} = [w^1\ w^2\ w^3]^T$, representing the kinematic variables conjugated to the effective cohesive stresses $\mathbf{s}$ in the expression of the free energy density Ψ and defined as the projection of the dimensionless relative displacements vector $\overline{\boldsymbol{\delta}}$ onto a structural vector $\mathbf{m^i}$ (see Figure 3). In matrix form:

$$\mathbf{w} = \mathbf{M}\overline{\boldsymbol{\delta}} \tag{9}$$

where:

$$\overline{\boldsymbol{\delta}} = \begin{bmatrix} \overline{\delta}^n \\ \overline{\delta}^s \end{bmatrix} = \begin{bmatrix} \frac{\delta^n}{\delta_0^n} \\ \frac{\delta^s}{\delta_0^s} \end{bmatrix} \tag{10}$$

being δ_0^n and δ_0^s the relative displacements at the onset of delamination, i.e. corresponding to t_0^n and t_0^s. $\mathbf{M}$ is the matrix gathering the components of the three structural vectors $\mathbf{m^i}$:

$$\mathbf{M} = \begin{bmatrix} \mathbf{m^1} \\ \mathbf{m^2} \\ \mathbf{m^3} \end{bmatrix} = \begin{bmatrix} a & 0 \\ b\sin\theta & b\cos\theta \\ b\sin\theta & -b\cos\theta \end{bmatrix} \tag{11}$$

being θ the angle defining the orientation of $\mathbf{m^2}$ and $\mathbf{m^3}$. As shown in Figure 3, $\mathbf{m^1}$ is aligned to $\mathbf{n^1}$ for symmetry considerations. The two unknown constants a and b are determined by imposing that the elastic strain energy density Ψ remains the same in passing from the direct to the effective variables, i.e.

$$\frac{1}{2}\mathbf{t}^T\boldsymbol{\delta} = \frac{1}{2}\left(s^1w^1 + s^2w^2 + s^3w^3\right) \tag{12}$$

From eqn. 12, one obtains:

$$a = (t_0^n\delta_0^n - t_0^s\delta_0^s\tan\alpha\tan\theta) \qquad b = \frac{t_0^s\delta_0^s}{2\cos\alpha\cos\theta} \tag{13}$$

Thus,

$$\begin{aligned} w^1 &= \overline{\boldsymbol{\delta}}^T\mathbf{m^1} = (t_0^n\delta_0^n - t_0^s\delta_0^s\tan\alpha\tan\theta)\,\overline{\delta}^n \\ w^2 &= \overline{\boldsymbol{\delta}}^T\mathbf{m^2} = \tfrac{t_0^s\delta_0^s}{2\cos\alpha\cos\theta}\left(\sin\theta\overline{\delta}^n + \cos\theta\overline{\delta}^s\right) \\ w^3 &= \overline{\boldsymbol{\delta}}^T\mathbf{m^3} = \tfrac{t_0^s\delta_0^s}{2\cos\alpha\cos\theta}\left(\sin\theta\overline{\delta}^n - \cos\theta\overline{\delta}^s\right) \end{aligned} \tag{14}$$

Based on the definitions 6 and 9 of effective stresses and relative displacements, the overall strain energy density can be decomposed into the sum of three distinct contributions, each one associated to a damage mode as:

$$\Psi = \frac{1}{2}\mathbf{t}^T\boldsymbol{\delta} = \underbrace{\frac{1}{2}s^1w^1}_{\Psi^1} + \underbrace{\frac{1}{2}s^2w^2}_{\Psi^2} + \underbrace{\frac{1}{2}s^3w^3}_{\Psi^3} \tag{15}$$

By exploiting the decomposition of eqn. 15, three effective strain energies Y^i released per unit growth of damage can also be defined through the state equations as:

$$\begin{aligned} Y^1 &= -\frac{\partial\Psi^1}{\partial d} = \frac{1}{2}\left(t_0^n\delta_0^n - t_0^s\delta_0^s\tan\alpha\tan\theta\right)\left\langle\overline{\delta}^n\right\rangle^2 \\ Y^2 &= -\frac{\partial\Psi^2}{\partial d} = \frac{1}{4}t_0^s\delta_0^s\left[\tan\alpha\tan\theta\left\langle\overline{\delta}^n\right\rangle^2 + \left\langle\overline{\delta}^s\right\rangle^2 + \left(\tan\alpha+\tan\theta\right)\overline{\delta}^n\overline{\delta}^s\right] \\ Y^3 &= -\frac{\partial\Psi^3}{\partial d} = \frac{1}{4}t_0^s\delta_0^s\left[\tan\alpha\tan\theta\left\langle\overline{\delta}^n\right\rangle^2 + \left\langle\overline{\delta}^s\right\rangle^2 - \left(\tan\alpha+\tan\theta\right)\overline{\delta}^n\overline{\delta}^s\right] \end{aligned} \tag{16}$$

It can be observed that:

$$Y^1 + Y^2 + Y^3 = \frac{1}{2}t_0^n\delta_0^n\left\langle\overline{\delta}^n\right\rangle^2 + \frac{1}{2}t_0^s\delta_0^s\left\langle\overline{\delta}^s\right\rangle^2 = Y \tag{17}$$

with $t_0^n = K\delta_0^n$ and $t_0^s = K\delta_0^s$. The decomposition of the strain energy release rate Y into its three components Y^i depends on the ratio $\frac{t_0^n\delta_0^n}{t_0^s\delta_0^s}$ and on the angles α and θ. In the applications, it will be assumed that:

$$\theta = \arctan\left(\frac{t_0^n\delta_0^n}{t_0^s\delta_0^s}\tan\alpha\right) \tag{18}$$

so that Y^1 is always positive for any positive value of δ^n. Under this hypothesis, either Y^2 or Y^3 can be negative, but their sum $Y^2 + Y^3 = \frac{1}{2}\left[\tan\alpha\tan\theta\left\langle\overline{\delta}^n\right\rangle^2 + \left\langle\overline{\delta}^s\right\rangle^2\right]$, representing the fraction of the strain energy release rate associated to the shear-dominated damage modes, is always positive.

An energy criterion is considered to express the damage activation function:

$$\varphi = \left(\frac{Y^1}{\chi_0^1+\chi^1}\right)^k + H(Y^2)\left(\frac{Y^2}{\chi_0^2+\chi^2}\right)^k + H(Y^3)\left(\frac{Y^3}{\chi_0^3+\chi^3}\right)^k - 1 \leq 0 \tag{19}$$

where $H()$ is the Heavyside function introduced to exclude possible negative contribution of Y^2 or Y^3 to damage activation, the exponent k is a parameter of the proposed cohesive model and $(\chi_0^i + \chi^i)$ represents the current threshold of the $i-th$ damage mode, being χ_0^i its initial value and χ^i an internal variable governing its evolution with damage and determining the shape of the softening branch. In this work, a model exhibiting a bilinear traction-separation law in pure Modes I and II (see Figure 5) is considered, although other choices of the functional form of the traction-separation curves (e.g. with an exponential strength decay) are in principle allowed. Figure 4 shows the damage activation surface at the onset of decohesion, for increasing values of the internal friction angle α and $k = 2$

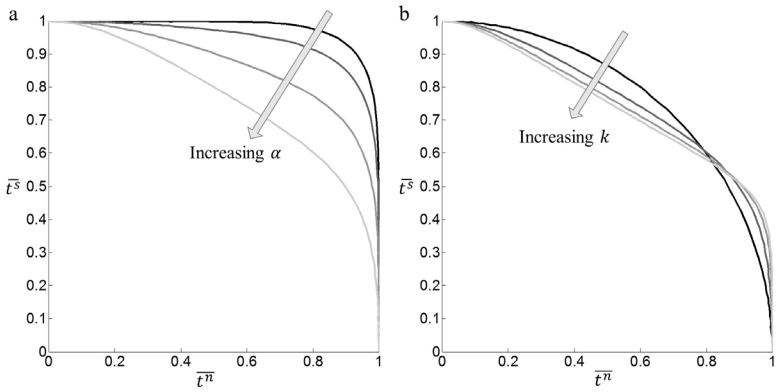

Figure 4: First activation domain: a) for increasing values of α and $k = 2$; b) for increasing values of k and $\alpha = 30°$

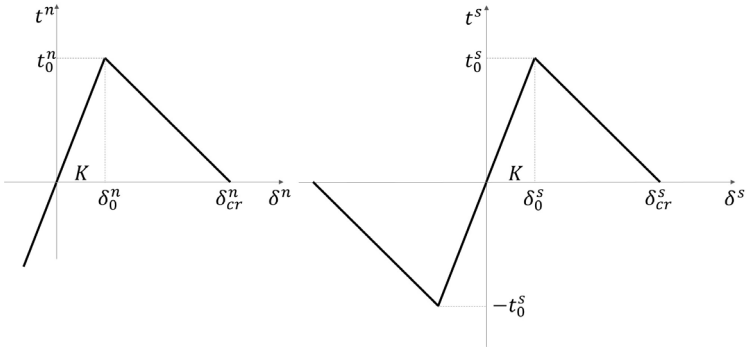

Figure 5: Bilinear cohesive laws in pure Modes I and II

(a) and for increasing values of the exponent k, while maintaining a constant value of the angle $\alpha = 30°$ (b).

The expressions of χ_0^i and χ^i for the bilinear law can be found by considering the behavior in pure loading Modes. At first, let us consider a pure Mode II case, characterized by $\delta^n = 0$ and $\delta^s \neq 0$. Under this hypothesis, it holds that (subscripts mI and mII denote pure Mode I and Mode II loading conditions):

$$\begin{aligned} Y_{mII}^1 &= 0 \\ Y_{mII}^2 &= \tfrac{1}{4} t_0^s \delta_0^s \left(\overline{\delta}^s\right)^s \\ Y_{mII}^3 &= \tfrac{1}{4} t_0^s \delta_0^s \left(\overline{\delta}^s\right)^s \end{aligned} \tag{20}$$

Because of the symmetry of the two shear dominated damage modes, it turns out that $Y_{mII}^2 = Y_{mII}^3$, $\chi_0^2 = \chi_0^3$ and $\chi^2 = \chi^3$. The initial thresholds χ_0^2 and χ_0^3 can be determined by imposing that the activation function is zero at the onset of delamination, i.e. for $\overline{\delta}^s = 1$. Thus,

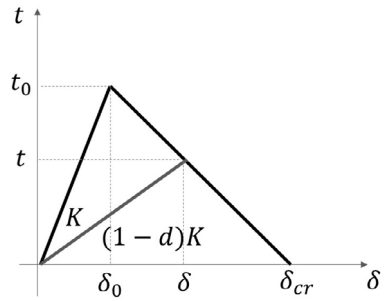

Figure 6: Pure mode bilinear law

$$\phi = \left(\frac{Y^2_{mII}|_1}{\chi^2_0}\right)^k + \left(\frac{Y^3_{mII}|_1}{\chi^3_0}\right)^k = 2\left(\frac{Y^2_{mII}|_1}{\chi^2_0}\right)^k - 1 = 0 \quad \rightarrow \quad \chi^2_0 = \chi^3_0 = 2^{\frac{1}{k}}\frac{1}{4}t^s_0\delta^s_0 \tag{21}$$

Analogously, by considering a generic point along the softening branch, it is possible to find the expressions of χ^2 and χ^3 as:

$$\phi = \left(\frac{Y^2_{mII}}{\chi^2_0+\chi^2}\right)^k + \left(\frac{Y^3_{mII}}{\chi^3_0+\chi^2}\right)^k - 1 = 0 \quad \rightarrow \quad \chi^2 = \chi^3 = 2^{\frac{1}{k}}\frac{1}{4}t^s_0\delta^s_0\left[\left(\overline{\delta}^s\right)^2 - 1\right] \tag{22}$$

If a pure mode case is considered, the relationship between the relative displacement and the damage variable can be obtained on the basis of purely geometrical considerations, given the triangular shape of the cohesive law depicted in Figure 6.

$$\delta = \frac{\delta_{cr}\delta_0}{\delta_{cr} - (\delta_{cr} - \delta_0)d} \tag{23}$$

By substituting eqn. 23 into eqn. 22, one obtains:

$$\chi^2 = \chi^3 = 2^{\frac{1}{k}}\frac{1}{4}t^s_0\delta^s_0\left[\frac{\delta^s_{cr}}{\delta^s_{cr} - (\delta^s_{cr} - \delta^s_0)\,d}\right]^2 - \chi^2_0 \tag{24}$$

While in pure Mode II one has $Y^1_{mII} = 0$, in a pure Mode I case, i.e. for $\delta^n \neq 0$ and $\delta^s = 0$, Y^2_{mI} and Y^3_{mI} are also non-zero:

$$\begin{aligned} Y^1_{mI} &= \tfrac{1}{2}\left(t^n_0\delta^n_0 - t^s_0\delta^s_0\tan\alpha\tan\theta\right)\left(\overline{\delta}^n\right)^2 \\ Y^2_{mI} &= \tfrac{1}{4}t^s_0\delta^s_0\left(\tan\alpha\tan\theta\overline{\delta}^n\right)^s \\ Y^3_{mI} &= \tfrac{1}{4}t^s_0\delta^s_0\left(\tan\alpha\tan\theta\overline{\delta}^n\right)^s \end{aligned} \tag{25}$$

At delamination onset (i.e. for $\overline{\delta}^n = 1$), it holds that:

$$\phi = \left(\frac{Y^1_{mI}|_1}{\chi^1_0}\right)^k + \left(\frac{Y^2_{mI}|_1}{\chi^2_0}\right)^k + \left(\frac{Y^3_{mI}|_1}{\chi^3_0}\right)^k - 1 = 0 \quad \rightarrow \quad \chi^1_0 = \frac{1}{2}\frac{\left(t^n_0\delta^n_0 - t^s_0\delta^S_0\tan\alpha\tan\theta\right)}{\left[1-(\tan\alpha\tan\theta)^k\right]^{\frac{1}{k}}} \tag{26}$$

while, by imposing that the activation function is zero for a generic dimensionless opening displacement $\overline{\delta}^n$, i.e.

$$\phi = \left(\frac{Y^1_{mI}}{\chi^1_0 + \chi^1}\right)^k \left(\frac{Y^2_{mI}}{\chi^2_0 + \chi^2}\right)^k + \left(\frac{Y^3_{mI}}{\chi^3_0 + \chi^2}\right)^k - 1 = 0 \tag{27}$$

one obtains:

$$\chi^1 = \frac{\left(t^n_0 \delta^n_0 - t^s_0 \delta^S_0 \tan\alpha \tan\theta\right)}{\left\{1 - \left[\left(\frac{\delta^n_{cr}}{\delta^s_{cr}} \frac{\delta^s_{cr} - (\delta^s_{cr} - \delta^s_0)d}{\delta^n_{cr} - (\delta^n_{cr} - \delta^n_0)d}\right)^2 \tan\alpha \tan\theta\right]^k\right\}^{\frac{1}{k}}} \frac{1}{2} \left(\frac{\delta^n_{cr}}{\delta^n_{cr} - (\delta^n_{cr} - \delta^n_0)d}\right)^2 - \chi^1_0 \tag{28}$$

The formulation of the proposed cohesive model is completed by the introduction of the evolution law, expressing the damage rate as:

$$\dot{d} = -\frac{\frac{\partial\phi}{\partial\delta^n}\dot{\delta}^n + \frac{\partial\phi}{\partial\delta^s}\dot{\delta}^s}{\frac{\partial\phi}{\partial d}} = \frac{\sum_{i=1}^3 \left(\frac{\partial\phi}{\partial Y^i}\frac{\partial Y^i}{\partial\delta^n}\right)\dot{\delta}^n + \sum_{i=1}^3 \left(\frac{\partial\phi}{\partial Y^i}\frac{\partial Y^i}{\partial\delta^s}\right)\dot{\delta}^s}{\sum_{i=1}^3 \left(\frac{\partial\phi}{\partial\chi^i}\frac{\partial\chi^i}{\partial d}\right)} \tag{29}$$

together with the classical loading/unloading conditions:

$$\phi \leq 0 \qquad \dot{d} \geq 0 \qquad \phi\dot{d} = 0 \tag{30}$$

Using a classical argument, based on the Clausius-Duhem inequality for isothermal processes, the mechanical dissipation can be proven to be always non-negative:

$$D = Y^1\dot{d} + Y^2\dot{d} + Y^3\dot{d} = \left(Y^1 + Y^2 + Y^3\right)\dot{d} = Y\dot{d} \geq 0 \tag{31}$$

The definition of the proposed cohesive model requires the following input parameters: the fracture energies G_{Ic}, G_{IIc} and the peak tractions t^n_0, t^s_0 in pure Modes I and II, the internal friction angle α and the exponent k appearing in the activation function ϕ. These parameters can be identified based on the results of standard experimental tests, i.e. one Double Cantilever Beam (DCB) test for pure Mode I, one End Notch Flexure (ENF) test for pure Mode II and a set of Mixed Mode Bending (MMB) tests [7] for varying mode-mixity ratio, from which a curve describing the evolution of the fracture energy with the mode mixity ratio can be constructed.

3 NUMERICAL EXAMPLES

The accuracy of the proposed model is assessed at a material point level by prescribing the two components of the relative displacement along different paths, for a number of different parameter sets.

3.1 Consistency tests: proportional path

Radial loading conditions with varying separation angles are enforced by imposing $\delta^n = (1-\beta)\,\gamma$ and $\delta^s = \beta\gamma$, γ being a multiplier linearly increasing from 0 to $\gamma_{max} = 0.1$ mm and $\beta \in [0,1]$ a parameter defining the mode-mixity. Pure Modes I and II are recovered for $\beta = 0$ and $\beta = 1$, respectively. Identical cohesive properties are here assumed for the pure Modes, considering $G_{Ic} = G_{IIc} = 0.1$ kJ/m^2 and $t^n_0 = t^s_0 = 6$ MPa.

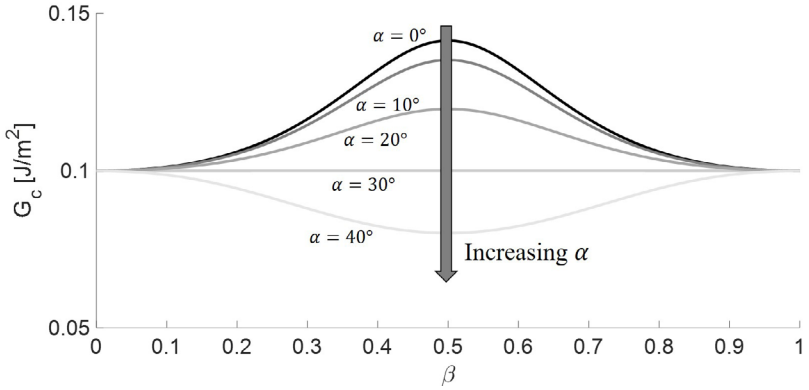

Figure 7: Fracture energy vs mode mixity for $k = 2$, $G_{Ic} = G_{IIc}$, $t_0^n = t_0^s$ for increasing values of angle α

Under these hypotheses, it is possible to show analytically that the softening branch is linear for any value of β (note that this is not the case for $\beta \neq 0$ and $G_{Ic} \neq G_{IIc}$, even when the traction-separation curves are bilinear in pure modes). Moreover, for an exponent $k = 2$ (i.e. quadratic damage activation surface), the response is symmetric with respect to $\beta = 0.5$, i.e. the response is the same for β_1 and $\beta_2 = 1 - \beta_1$. Figure 7 shows the evolution of the overall fracture energy G_c with the mode mixity parameter β, computed as the sum of the areas beneath the traction-separation curves. Increasing the internal friction α has the effect of reducing the peak value, without changing its position because of symmetry. It is noteworthy that for $\alpha = 30°$, the model is able to reproduce the case of constant fracture energy. This result can be found also analytically, by imposing that the activation function is zero at the onset of delamination and at complete decohesion, so that the two corresponding values of γ_0 and γ_{cr} are obtained:

$$\gamma_0 = \frac{\delta_0}{\left[(1-\beta)^4 + 6\beta^2 (1-\beta)^2 \tan\alpha^2 + \beta^4\right]^{\frac{1}{4}}}, \qquad \gamma_{cr} = \gamma_0 \frac{\delta_{cr}}{\delta_0} \tag{32}$$

For $\alpha = 30°$, one obtains:

$$\gamma_0 = \frac{\delta_0}{\sqrt{1 - 2\beta + 2\beta^2}}, \qquad \gamma_{cr} = \frac{\delta_{cr}}{\sqrt{1 - 2\beta + 2\beta^2}} \tag{33}$$

The fracture energy turns out to be independent of β, i.e.:

$$G_c = \frac{1}{2} K (1-\beta)^2 \gamma_0 \gamma_{cr} + \frac{1}{2} K \beta^2 \gamma_0 \gamma_{cr} = \frac{1}{2} K \delta_0 \delta_{cr} = \text{const.} \tag{34}$$

3.2 Consistency test: non-proportional path

The non-proportional, zig-zag loading path proposed in [12] and depicted in Figure 8a is considered in this example. The adopted cohesive properties are listed in Table 1. Figure 8b shows the evolution of the damage variable: since a monotonically increasing separation is applied, the damage increases monotonically as expected. The resulting traction-separation curves are shown in Figure 9.

Table 1: Non proportional zig-zag path: cohesive properties

t_0^n MPa	t_0^s MPa	G_{Ic} $\frac{J}{m^2}$	G_{IIc} $\frac{J}{m^2}$	α	k
10	10	100	100	30	4

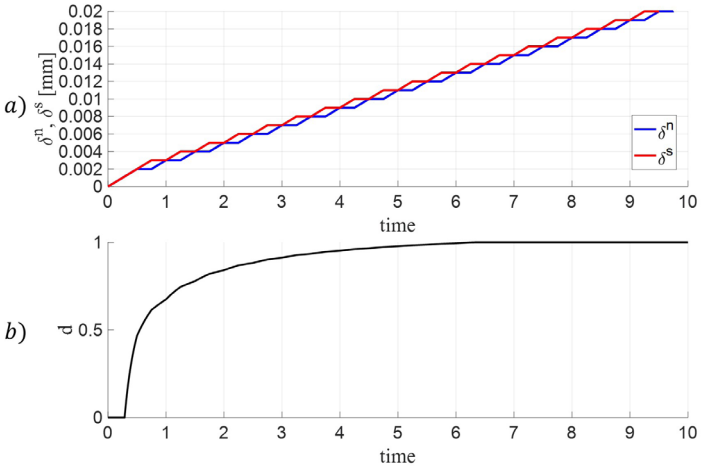

Figure 8: Zig-zag path: a) relative displacement history, b) damage variable evolution.

3.3 Mixed-mode bending (MMB) tests

The experimental data of the Mixed Mode Bending (MMB) tests performed by Reeder [8] on three different fibre reinforced composites, namely AS4/PEEK, AS4/3501-6 and IM7/977-2, are here considered to assess the capability of the proposed model to reproduce the mixed-mode behaviour over the full range of mode-mixity ratios. The adopted cohesive properties are reported in Table 2. The internal friction angle α and the exponent k are the values that guarantees the best fitting of the experimental data. The fracture energy is computed as the sum of the areas beneath the normal and shear traction-separation curves, obtained with a series of radial paths in the $\delta^n - \delta^s$ plane, with increasing mode-mixity ratio. In figure 10 the numerical prediction of the fracture energy for varying mode-mixity ratio is compared with the experimental data and with the results obtained with a Power Law, whose exponents have been calibrated in [8]: the dots corresponds to the experimental points, the red dashed lines are obtained with the empirical Power Law and the solid lines are the results of the present model. In all the three cases, the model is able to reproduce correctly the non-monotonic growth of the fracture energy with the mode mixity ratio and the numerical results are very close to the best fitting obtained by Reeder, without the need of adopting any empirical law.

4 CONCLUSIONS

A new isotropic damage cohesive model has been proposed for the simulation of delamination under mixed-mode loading conditions. The model is based on the introduction of

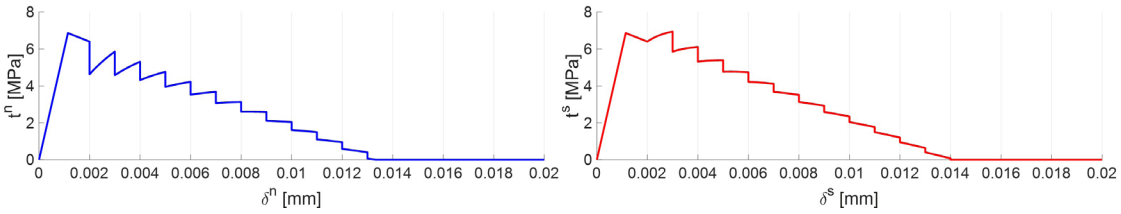

Figure 9: Zig-zag path: traction-separation laws.

Table 2: Cohesive properties

	t_0^n MPa	t_0^s MPa	G_{Ic} $\frac{J}{m^2}$	G_{IIc} $\frac{J}{m^2}$	α	k
AS4/PEEK	80	100	779	1142	24	1.6
AS4/3501-6	45	48	90	600	25	12
IM7/977-2	70	130	310	1410	28	12

an internal friction dissipation mechanism, which allows to handle the coupling between normal and shear damage modes. The resuting mixed-mode fracture energy is the outcome of modes interaction, without the need to define a-priori any empirical law. The model is thermodynamically consistent, even under arbitrary non proportional loading paths, with variable mode ratio.

5 Acknowledgements

The financial support of Tetra Pak Packaging Solutions is gratefully acknowledged.

REFERENCES

[1] Hibbs, M.F. and Bradley, W.L. Correlations between micromechanical failure processes and the delamination toughness of graphite/epoxy systems. *Fractography of Modern Engineering Materials: Composites and Metals, ASTM International* Vol. 948, (1987)

[2] Greenalgh, E.S. and Rogers, C. and Robinson, P. Fractographic observations on delamination growth and the subsequent migration through the laminate. *Composites Science and Technology* (2009) **69**:2345–2351.

[3] Marat-Mendes, R. and de Freitas, M. Fractographic analysis of delamination in glass/fibre epoxy composites. *Journal of Composite Materials* (2013) **47**:1437–1448.

[4] Benzeggagh, M.L. and Crews, J.H. Measurement of mixed-mode delamination fracture toughness of unidirectional glass/epoxy composites with mixed-mode bending apparatus. *Composites Science and Technology*, (1996) **56**:439–449.

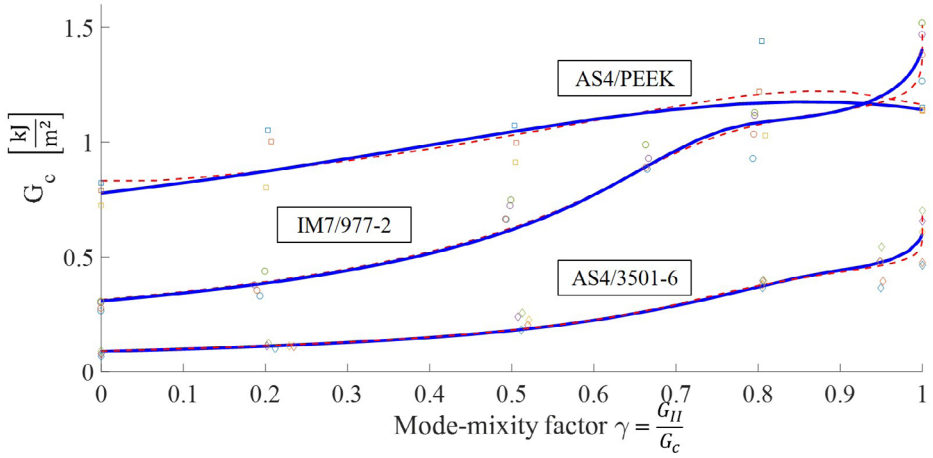

Figure 10: Experimental vs numerical mixed-mode fracture energies. Dots: experimental data [8]. Dashed line: Power Law [8]. Solid line: result of the present model.

[5] Davidson, B.D. and Zhao, W. An accurate mixed-mode delamination failure criterion for laminated fibrous composites requiring limited experimental input. *Journal of Composite Materials* (2007) **41**: 679–702.

[6] Mathews, M. J., and Swanson, S. R. Characterization of the interlaminar fracture toughness of a laminated carbon/epoxy composite. *Composites Science and Technology* (2007) **67**: 1489–1498.

[7] Reeder, J.R. and Crews, J.H. Mixed-mode bending method for delamination testing. *AIAA Journal* (1990)**28**:1270-1276.

[8] Reeder, J.R., An Evaluation of Mixed-Mode Delamination Failure Criteria. *NASA Technical Reports* (1992) **ID:19920009705**:1-50.

[9] Camanho, P.P and Davila, C.G. and de Moura, M.F. Numerical Simulation of Mixed-mode Progressive Delamination in Composite Materials. *Journal of Composite Materials* (2003) **37**:1415–1438.

[10] Van den Bosch, M.J. and Schreurs, P. J. G. and Geers, M. G. D. An improved description of the exponential Xu and Needleman cohesive zone law for mixed-mode decohesion. *Engineering Fracture Mechanics* (2006) **73**:1220–1234.

[11] Park, K. and Paulino, G. H. and Roesler, J. R. A unified potential-based cohesive model of mixed-mode fracture. *Journal of the Mechanics and Physics of Solids* (2009) **57**:891-908.

[12] Park, K. and Choi, H. and Paulino, G. Assessment of cohesive traction-separation relationships in ABAQUS: a comparative study. *Mechanics Research Communications* (2016) **78**:71–78